



HAL
open science

Joint inversion of marine magnetotelluric and gravity data incorporating seismic constraints: Preliminary results of sub-basalt imaging off the Faroe Shelf

Marion D. Jegen, Richard W. Hobbs, Pascal Tarits, Alan D Chave

► To cite this version:

Marion D. Jegen, Richard W. Hobbs, Pascal Tarits, Alan D Chave. Joint inversion of marine magnetotelluric and gravity data incorporating seismic constraints: Preliminary results of sub-basalt imaging off the Faroe Shelf. *Earth and Planetary Science Letters*, 2009, 282 (1-4), pp.47-55. 10.1016/j.epsl.2009.02.018 . insu-00422104

HAL Id: insu-00422104

<https://insu.hal.science/insu-00422104>

Submitted on 1 May 2024

HAL is a multi-disciplinary open access archive for the deposit and dissemination of scientific research documents, whether they are published or not. The documents may come from teaching and research institutions in France or abroad, or from public or private research centers.

L'archive ouverte pluridisciplinaire **HAL**, est destinée au dépôt et à la diffusion de documents scientifiques de niveau recherche, publiés ou non, émanant des établissements d'enseignement et de recherche français ou étrangers, des laboratoires publics ou privés.

Joint inversion of marine magnetotelluric and gravity data incorporating seismic constraints

Preliminary results of sub-basalt imaging off the Faroe Shelf

Marion D. Jegen^{a,*}, Richard W. Hobbs^b, Pascal Tarits^c, Alan Chave^d

^a IFM-GEOMAR, Wischhofstr. 1-3, 24148 Kiel, Germany

^b Dept. of Earth Science, University of Durham, South Road, Durham DH1 3LE, UK

^c Université de Bretagne Occ., Place Nicholas Copernic, 29280 Plouzane, France

^d Woods Hole Oceanographic Institution, Woods Hole, MA 02543, USA

Breakup of the North Atlantic during the early tertiary was accompanied by widespread and massive magmatism, resulting in the coverage of large areas of the North Atlantic with flood basalts. These flood basalts hamper seismic investigations of underlying sequences and thus the understanding of the rifting, subsidence and evolution of the margin which, in turn, increases the risk for hydrocarbon exploration. In this paper we present a methodology for the simultaneous joint inversion of diverse geophysical datasets, i.e. free air gravity and magnetotelluric soundings (MT) using seismic a priori constraints. The attraction of the joint inversion approach is that different geophysical measurements are sensitive to different properties of the sub-surface, so through joint inversion we significantly reduce the null space and produce a single model that fits all datasets within a predefined tolerance. Using sensitivity analysis of synthetic data, we show how each data set contains complementary important information of the supra and sub-basalt structure. While separate inversions of individual datasets fail to image through the basalt layer, our joint inversion approach leads to a much improved sub-basalt structure. Application of the joint inversion algorithm to satellite gravity data and MT data acquired on the FLARE10 seismic line south west of Faroe islands supports the existence of a 1 km to 2 km thick low velocity region that might be indicative of the existence of a sedimentary basin underneath the basalt layer. Though in this paper we demonstrate the use of joint inversion on a sub-basalt target, we believe it has wider applicability to other areas where conventional seismic imaging fails.

1. Introduction

The geology of the sub-surface affects physical properties, such as density, seismic velocity or electrical resistivity. Conversely, estimates of the physical properties of the Earth can be obtained through the process called inversion from geophysical data such as gravity, seismic or electromagnetic profiles respectively. Inversion of geophysical data of any kind is inherently non-unique, so a variety of Earth models may fit the data equally well. This is due to the fact that: a) the data are typically measured on the surface only, while physical properties vary in three dimensions; b) the geophysical response is insensitive to certain features due to the fact that the resolution capability of the data at a given depth is low or the changes of the physical parameter due to particular features are small; c) data measurements contain noise and are band-limited so there is an inherent uncertainty for any given datum; and d) our models are simplifications of the true Earth.

There is inherent non-uniqueness in the different methods, based on the physics of the responses. While there are usually many models or a large part of the model space which may fit a given gravity data set, the number of model fitting magnetotelluric (MT) data is small and yet smaller again for seismic data. While this is the general case, it is still model dependent. Sub-basalt imaging is one of the applications or type models in which traditional seismic data have proven to be less effective (e.g. Wombell et al., 1999; White et al., 1999). More sophisticated seismic data acquisition and analyses, such as two-ship data acquisition, refraction analysis of long offset data or low frequency information in reflection data (Ziolkowski et al., 2003; White et al., 2008) are needed to obtain any constraint on the seismic velocity variations underneath the basalt.

Geophysical data are sensitive to property variations on different scales and often contain complementary information. The key problem is how optimally synthesizing the information obtained by various methods. Comparison of models derived from inversion of a single data type may be misleading since these models may only partially represent the true model due to the non-uniqueness of the response. So, how can one most efficiently combine the complementary information content in different data? One approach is simultaneously inverting all of the

* Corresponding author. Tel.: +49 431 600 2560; fax: +49 431 600 2915.

E-mail addresses: mjegen@ifm-geomar.de (M.D. Jegen), r.w.hobbs@durham.ac.uk (R.W. Hobbs).

geophysical data in a process called joint inversion. In a joint inversion approach, a misfit is calculated for each type of input data for a common model, and these misfits are combined within the inversion program to drive improvements in the model fit. Hence the advantage of joint inversion is more flexibility over the relative influences of each data type and their interrelationships.

This technique has been used in the past with success. Vozoff and Jupp (1975) developed a scheme to invert DC resistivity and EM data, both of which measure the same physical property, the electrical resistivity, for a layered model. This concept has been successfully used in a variety of studies (e.g. Schmutz et al., 2000) and also in the inversion of seismic data using both reflected and refracted energy to constrain velocity structure (e.g. Trinks, 2005). These approaches employ the same methodologies and are still typically limited to deriving a single property of the sub-surface, though in some cases this may constrain several properties, e.g. pre-stack inversion of seismic data that can simultaneously produce models for compressional- and shear-wave velocities and density.

Several attempts have been made to invert data sets measuring different physical properties. These have mainly been focused on finding a common structural feature in the model (Haber and Oldenburg, 1997; Gallardo and Meju, 2003; Musil et al., 2003). In these cases the scientists have combined seismic or georadar data which both contain significant structural information with other geophysical data yielding a considerable improvement in data interpretation.

Here we report on a joint inversion approach, which capitalises on the different strengths of the three types of geophysical data: gravity; MT and reflection seismics. The algorithm we develop is a joint inversion of electromagnetic and gravity data using a priori constraints derived from seismic data. The research was motivated by the sub-basalt imaging issues for the north-west European margin, where potentially oil-bearing sub-basalt sediments are of vital interest for continued exploration and production of hydrocarbons. Traditional seismic imaging of the area delivers a sharp picture of the supra-basalt sediment sequence and top of the basalt, however, sub-basalt imaging is severely limited (Maresh and White, 2005). Other types of geophysical data contain complementary information. For MT methods the highly resistive basalt layer is transparent, and the response is mainly governed by the low resistivity sediments above and beneath the basalt. Gravity measurements on the other hand are particularly sensitive to the high density basalt layer and top basement structure and less sensitive to lower density sedimentary layers.

The two integrative methods, i.e. magnetotellurics and gravimetry, do not contain strong structural information, yet hold the most information about the sub-basalt sediments and basement in the models considered here, so we chose to develop a joint inversion code not based on common structure but through a linkage of the physical parameters density, velocity and electrical resistivity. Therefore a prerequisite of our approach to the joint inversion problem is the capability to express the common Earth model simultaneously as electrical resistivity, seismic velocity and density distribution. While analytical conversion between some physical properties (e.g. Wyllie et al., 1958) may exist for special settings, in general it is impossible to find relationships that are generally valid. We therefore resort to using commercial and ODP borehole data in the region and develop empirical relationships between the physical properties.

In this paper, we use a representative Earth model to investigate quantitatively the complementary information content of the various geophysical responses. Next we investigate to what degree the Earth model may be retrieved from the calculated synthetic geophysical responses and we compare inversion results from single methods and joint inversion results. Finally, we illustrate the capabilities of the joint inversion approach on sample MT, gravity and seismic data collected on the Faroes shelf.

2. Physical property relationship

Fig. 1a shows compressional seismic velocity v plotted against the electrical resistivity r derived from induction logs for ODP borehole 642e

gathered in the Voring basin off the Norwegian coast and a commercial borehole dataset gathered off the Faroes shelf. Fig. 1b depicts seismic velocity versus density data d for the ODP borehole (density values for the commercial borehole have been omitted due to strong scattering and noise). The raw data plotted in Fig. 1a and b exhibits some scatter that is partly due to noise in the measurements and/or local effects within the immediate vicinity of the borehole, and which actually bear little influence on the response of integrative methods such as gravimetry and MT. A correlation between the rock parameters is yet easily visible. The observed range of density is very small. The range of seismic velocity of one order of magnitude is also relatively small and varies between 1.5 km/s, the velocity in water and 6.5 km/s, the velocity of basalt. The electrical resistivity on the other hand changes over two orders of magnitude.

In this region, electrical conduction is caused by electrolytes, i.e. fluids, in the rocks; electrical resistivity is therefore dependent on porosity but also on connectivity of the pore space. The latter dependency explains the change in slope observed in the seismic velocity/resistivity relationship. The electrical bulk resistivity is small and varies slowly in the low velocity region since connected fluid pathways exist. At a critical point, corresponding to a seismic velocity of about 3 km/s to 3.5 km/s, the compaction is sufficiently high such that the pore space starts to become disconnected. The changes in the bulk electrical resistivity are then more pronounced, and increases in the seismic velocity, or compaction are reflected by rapidly increasing resistivity values. For a first approximation we fit two lines:

$$\text{for } v < 3600 \text{ m/s} : \log_{10}(\rho) = 1.20 * \log_{10}(v) - 3.86 \quad (1a)$$

$$\text{for } v > 3600 \text{ m/s} : \log_{10}(\rho) = 6.46 * \log_{10}(v) - 22.57, \quad (1b)$$

corresponding to the lower and higher velocity regions, where velocity and density units are given in m/s and resistivity in $\Omega \cdot m$.

For the velocity v and density d relationship of the sub-surface rocks a simple linear fit was sufficient, given by:

$$d = 1.700 + 2.0 \times 10^{-4} * v \quad (2)$$

with density in g/cm^3 and velocity and density of saltwater layer set to 1500 m/s and 1 g/cm^3 respectively.

The fitting of the borehole data is crude, but it captures the essence of rock property relationships in such a setting, which are characterized by increasing velocities giving rise to increasing electrical resistivities and densities. Investigations of the sensitivity of this relationship on a 1D joint inversion showed that the true model structure is recovered if synthetic MT and gravity data generated using Eqs. (1a), (1b) and (2) are inverted using rock property relationships shifted to the upper or lower limit of the scatter in Fig. 1. The presence of sedimentary structure beneath the basalt layer could still be resolved. Thus, the crude rock property approximation used here is sufficient to develop a first step towards the development and understanding of joint inversion of different geophysical data; however, it needs to be refined in future.

3. Geophysical response to sample sub-basalt Earth model

A 2-D Earth model developed as part of the EU-SIMBA project (Martini et al., 2005) was used to calculate synthetic geophysical responses for the testing and evaluation of the joint inversion strategy. This model represents a sedimentary structure that includes an extrusive basalt layer underlain by a basement. Fig. 2a shows the 2-D model using its original physical parameterisation in seismic velocity. This model was converted into resistivity and density models using Eqs. (1a), (1b) and (2). Since MT and gravity yield integrated responses over the whole model, the detailed model as shown in Fig. 2a is unnecessary, so we use a simplified model (Fig. 2b) where the heterogeneous basalt layers are replaced

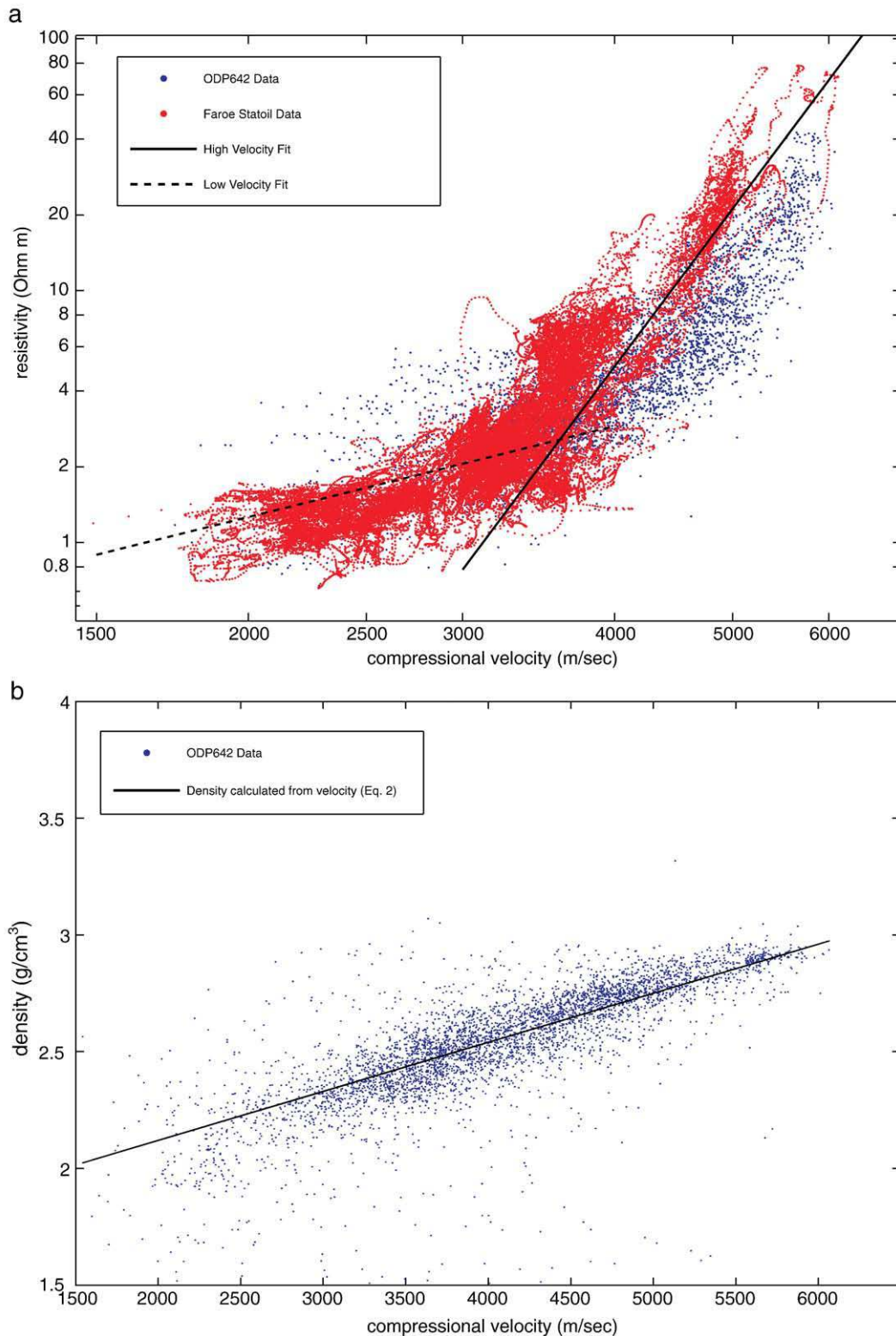


Fig. 1. a) Compressional velocity versus electrical resistivity for ODP642 borehole in the Voring basin and a Statoil borehole off the Faroe shelf. Solid and dotted lines denote relationship between velocity and electrical resistivity derived from linear fits of borehole data for low and high velocities. b) Compressional velocity versus density for ODP642 borehole in the Voring basin. Solid line denotes relationship between velocity and density derived from linear fit.

by homogeneous layers with averaged properties. Also, the structure was blocked to reduce the number of parameters to accelerate the inversion. In the subsequent sections we will discuss the various geophysical responses to the model and the sensitivity to structural elements.

3.1. Seismic response

The velocity model was used to compute synthetic seismic data using an elastic finite-difference staggered grid scheme of 4th order in space and 2nd order in time, using a stress-velocity formulation and

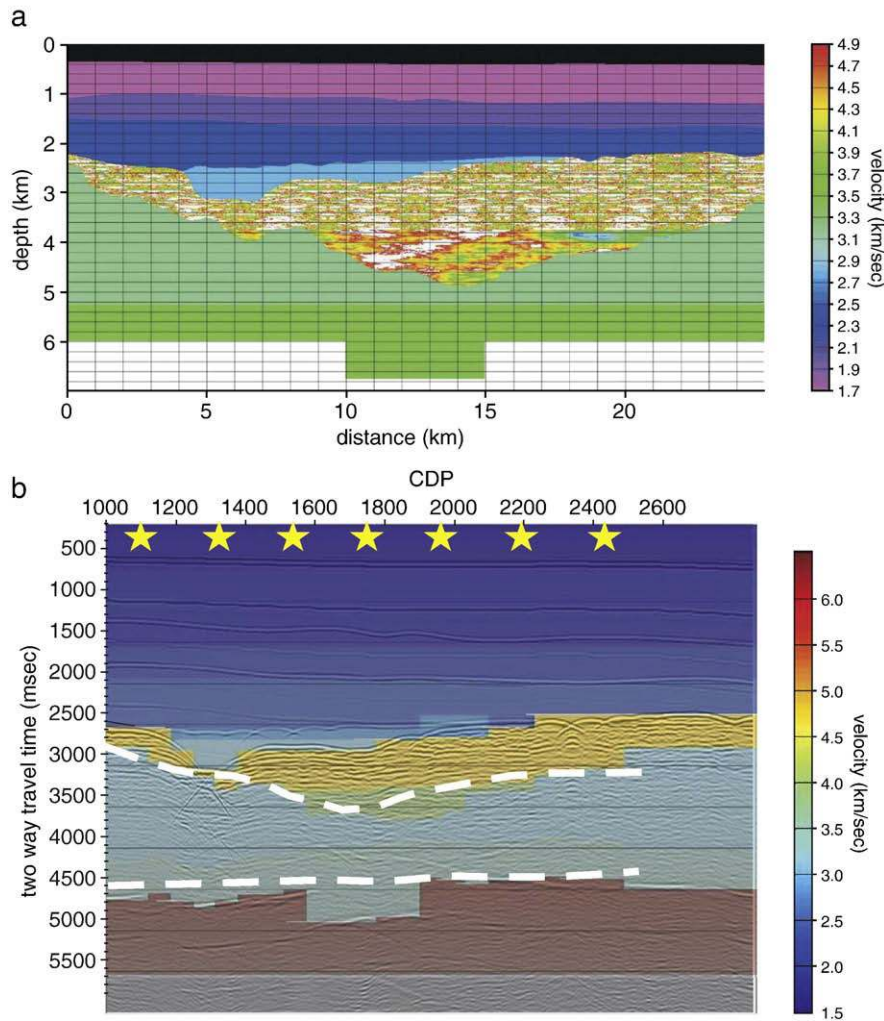


Fig. 2. a) Synthetic sub-basalt model derived in SIMBA project expressed in seismic velocity. Purple and blue colours denote supra-basalt sediments, green colours denote sub-basalt sediments, and white colour denotes the basement. The basalt layer between these sediment layers is heterogeneous. b) Gray scale background depicts synthetic travel time section produced from model shown in Fig. 1a. Overlay in colour shows model with simplified structure where heterogeneous basalt has been replaced with a two layered homogeneous basalt. This model is used in 2D MT and gravity forward modelling where resistivities and densities are then calculated from velocities using Eqs. (1a), (1b) and (2). In the overlay, the simplified model is expressed in velocities and shown in two way travel time instead of depth. Heavy dashed line show bottom of basalt layer and basement depth as derived from 1D joint inversion of synthetic 2D MT TM mode and gravity data (see Fig. 4). The locations of the MT stations used in the inversion are marked as yellow stars.

an efficient optimal absorbing boundary condition (Peng and Toksoz, 1995) to the sides and bottom and a reflecting boundary at the top to generate free-surface multiples as seen in real data. The shots, at 25 m spacing, were recorded on an 800 channel receiver array over the offset range of 0 to 10 km. Seismic data processing consisted of: sorting to common mid-point gathers; picking the stacking velocity function (every 2.5 km); normal moveout correction; top and inner trace mute (to suppress multiples sub-basalt); stack; and migration (Fig. 2b). As is common with real seismic data, the supra-basalt section is well defined with a good recovery of velocity structure down to and including the top basalt interface. Below this, the image is confused, identification of the base basalt is not clear and several spurious events exist in the sub-basalt region that could be misinterpreted as sedimentary structure or top basement.

3.2. MT response

The magnetotelluric (MT) method was developed by Cagniard (1953), Price (1962) and others. For the 2D model used in this paper, the Maxwell equations which govern the EM response decouple into two modes, the TE and TM mode, corresponding to a response due

to currents along or across strike. The TE and TM mode responses were calculated using a finite-difference code (Tarits, 1984) with a lateral cell size of 1 km for seven equi-spaced stations across the model. The modelled frequencies range from 1 to 10^{-5} Hz and correspond to the frequency range currently measurable at the seafloor for an ocean depth of 1 to 2 km and to the real data example used later in the paper. In this model, there are no large scale vertical contacts, so the difference in the responses for the two modes is small, indicating that we can invert data from each station with 1-D layered models. The TM mode response is shown in Fig. 3a and exhibits a smooth variation with frequency. It is characterized by an increase of apparent resistivity from $1 \Omega \text{ m}$ indicative of the upper sediment layers at high frequencies to $100 \Omega \text{ m}$ indicative of the basement at low frequencies. Lateral changes in the response in the frequency range of 10^{-2} to 10^{-5} Hz indicate that these frequencies penetrate into and through the laterally varying basalt structure. However, the low frequency range at which the structure is visible and the relatively subtle resistivity variations in the model indicate that the resolving power of the method is not high and that the MT response alone may not be capable of resolving the structure to a sufficiently.

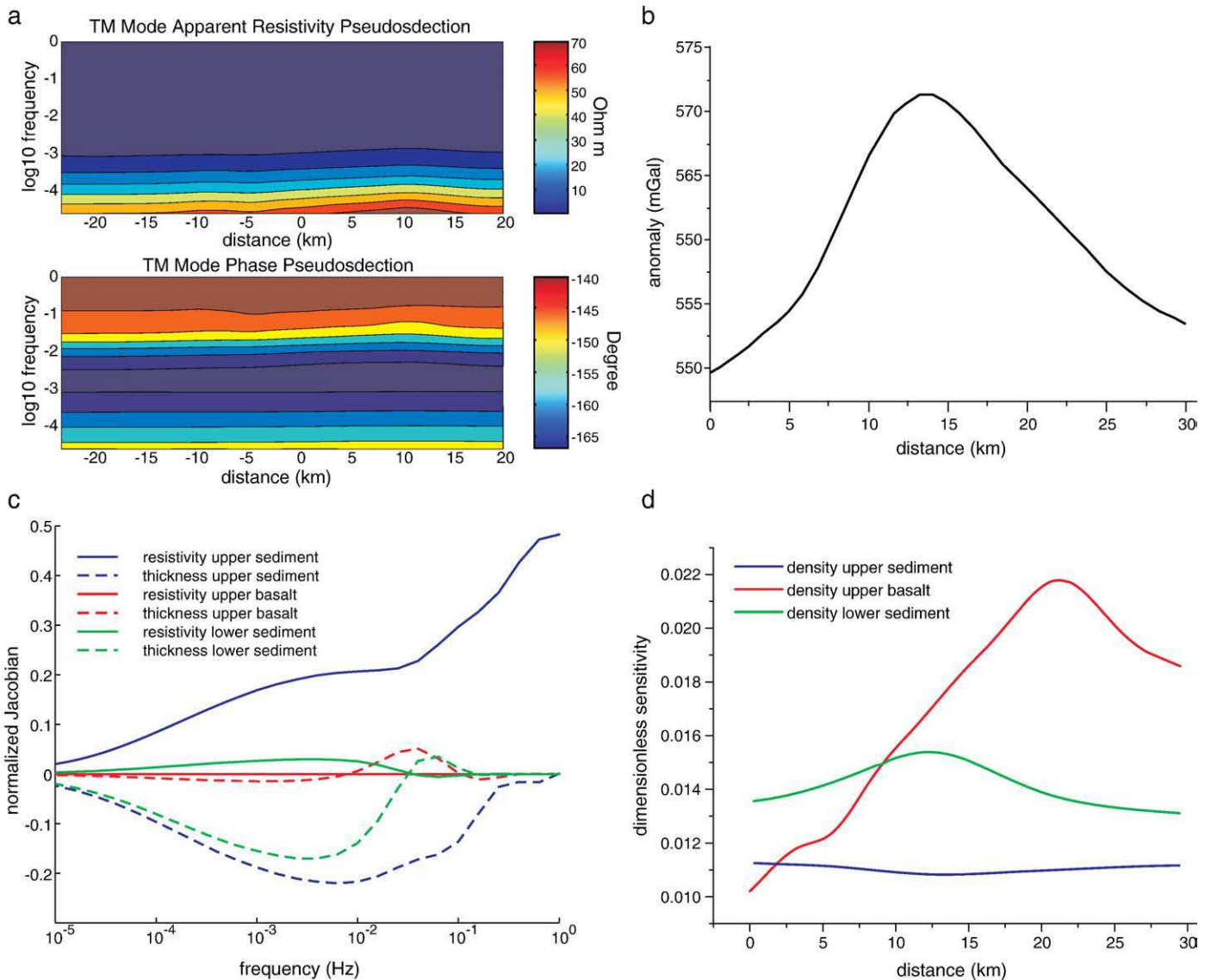


Fig. 3. (a) 2D TM mode response based on simplified model shown in Fig. 2b. For the 2D MT forward model, velocities have been converted to electrical resistivities using Eqs. (1a) and (1b). (b) 2D gravity anomaly based on simplified model shown in Fig. 2b. For the 2D gravity forward model, velocities have been converted to densities using Eq. (2). (c) Normalized Jacobian of MT amplitude response between 10⁻⁵ and 1 Hz for changes in thickness and resistivity of a 1D layered model derived from the centre of synthetic model shown in Fig. 2b. (d) Normalized sensitivity of gravity response to 2D density model based on simplified model shown in Fig. 2b.

3.3. Gravity response

The response has been calculated using the 2D GravMag software available from the British Geological Survey. The shape of the anomaly (Fig. 3b) shows an increase in the gravity response approximately over the centre of the model, where the high density basalt structure is thickest and sediment sections are the thinnest.

3.4. Model sensitivity

Derivatives of the response with respect to model parameters allow an assessment of the sensitivity of the MT or gravity response to elements of the structure. We plot the Jacobian for each model element, normalised by the original response and model parameter. While the absolute value itself is not of much significance, it allows us to compare the relative sensitivity to certain model elements within each method and assess which elements a response is most sensitive to. Fig. 3c shows the change of a 1-D response corresponding to a layered model obtained at the middle of the 2-D model. For the MT

data, the sensitivity to the upper sedimentary layers dominates the response, since the layers have low resistivity and hence a large amount of current will be induced causing a strong MT signal. The response is also relatively sensitive to the low resistive sediment layer below the basalt structure, although the overall sensitivity is smaller since the layer and its induced currents are further away from the measurement site. Due to the high resistivity of the basalt layer, the sensitivity of the response is virtually zero to changes in the resistivity in this part of the structure. There is sensitivity to changes in the thickness of the basalt layer. This is due to a change in thickness of the basalt layer causing a corresponding change to thickness of the low resistivity sediment layer above or beneath the basalt layer.

For the 2D gravity data, the sensitivity is largest to the high density basalt structures, while sensitivity to the approximately constant thickness lower density supra-basalt sedimentary layers is comparatively small (Fig. 3d). There is some sensitivity to the bottom sediment layer because of its 2-D structure. The model sensitivity study shows, that sensitivity of MT and gravity data to structural elements is complementary. The MT data are to the first degree sensitive to the

sedimentary structure and the gravity response to the basalt layer. Therefore the gravity response is ideal to supply additional constraints for this model where sensitivity is lacking from the MT response.

4. Joint inversion of gravity and MT data with a priori seismic constraints

We have developed a 2-D joint inversion code which consists of a full 2-D gravity calculation (thick prism formulae, e.g. Telford et al., 1976) combined with a quasi 2-D MT calculation consisting of a succession of 1-D layered MT models underneath each station. This approximation is justified by the particular geological setting and the forward 2-D MT response that showed only small lateral variations. An advantage of this approximation is that it allows us to avoid the

complexity of incorporating a full 2D MT code, while still allowing us to test the hypothesis that joint inversion may be applied successfully to sub-basalt imaging and whether further developments are warranted. In this initial inversion code we invert simultaneously for the density and resistivity value and layer thickness under all stations. In the misfit calculations we allow different weighting for the MT and gravity data misfit. This weighting is necessary so that the misfits for each data type have comparable values and thus carry the same weight in the inversion process. The data used in the inversion calculation consists of the 2-D MT TM mode data and the gravity data. We chose data from 7 equally spaced stations for the inversion study (see Fig. 2b).

Fig. 4a shows the discretisation of the inversion model, consisting of 7 layered strips underneath each station and populated with

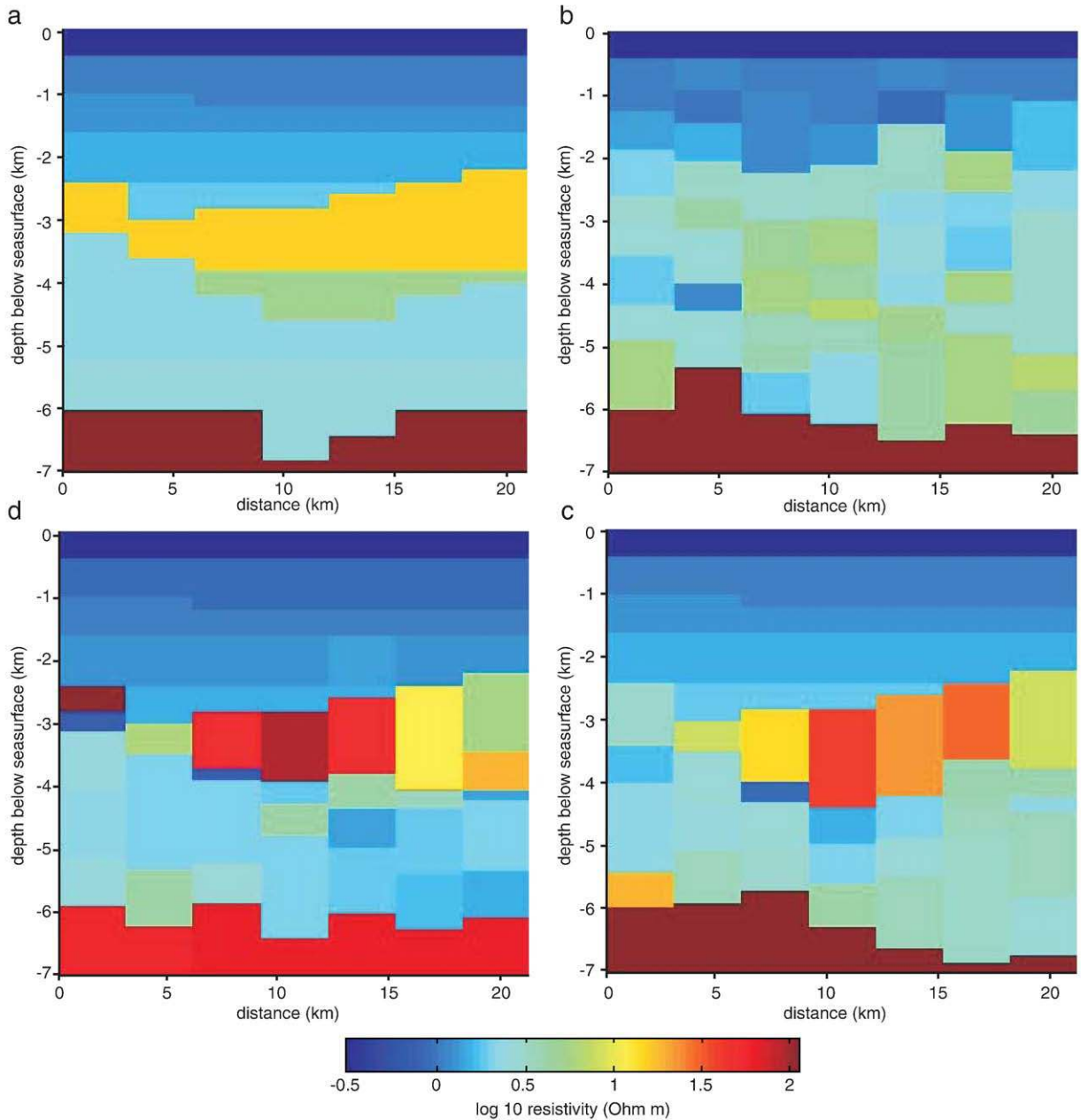


Fig. 4. Clockwise from top left: (a) Resistivity section derived from original model (Fig. 2b) for 7 equally spaced stations along profile. (b) Model derived from 2D synthetic MT response (calculated according to model shown in Fig. 2b) by 1D layered inversion underneath 7 stations. (c) Model derived from 2D synthetic MT response (calculated according to model shown in Fig. 2b) by 1D layered inversion underneath 7 stations using seismic a priori constraints for supra-basalt sediments. (d) Model derived from 2D synthetic MT response and 2D gravity data by joint 1D MT and 2D gravity inversion underneath 7 stations using seismic a priori constraints for supra-basalt sediments. Base of basalt and basement depth from this inversion result have been converted to two way travel time and are shown as heavy dashed line on seismic section in Fig. 2b.

averaged resistivities of the original model (Fig. 2b). The starting model for the inversion consists of the upper sedimentary sequence derived from the seismic data underlain by a $2 \Omega \text{ m}$ half-space (Fig. 4a). Fig. 4b depicts results of the inversion of the MT data only, without the use of seismic a priori information. The inversion result shows, that the MT data are capable of recovering the basement, and also to some extent the top of the basalt layer is imaged by a general increase in resistivity at a depth of around 2 km; however, it lacks any structural information about the basalt layer itself. Fig. 4c shows the inversion results if the MT data and seismic a priori information are

considered in the inversion process. The basalt layer is now visible, however its thickness and the depth to the basement are still not recovered in detail. The result is improved by the addition of the gravity data in the inversion process (Fig. 4d). The estimation of the basalt layer thickness as well as the depth to the basement is now in better agreement with the original model. In the region where there are variations in the basement, the derived model deviates from the true model in thickness and resistivity of the basalt structure as well as depth to the basement. We believe that this is a consequence of the substitution of the 2-D MT response by the quasi 2-D response

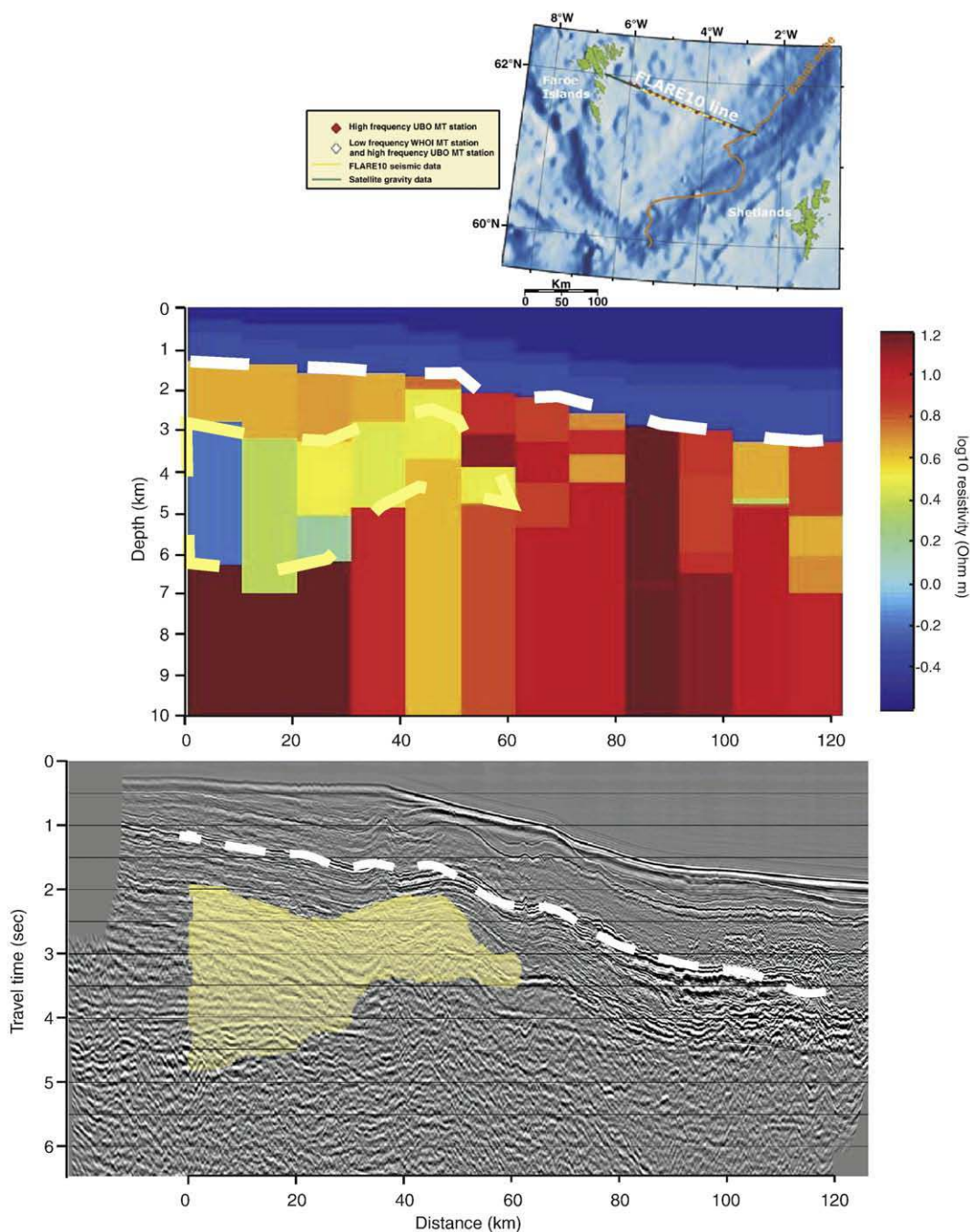


Fig. 5. Insert shows map of the survey layout east of Faroe islands. Upper panel: Resistivity depth section derived from 2D gravity/1D MT joint inversion. Data of 12 MT stations (stations 5 to 16), satellite gravity data together with supra-basalt sediment depth (dashed white line) derived from seismic data were used in the inversion. Dashed yellow line encircles region of low resistivity interpreted to be caused by sedimentary rich sequences. Bottom panel: Seismic travel time section of the Flare10 data, from which depth of supra-basalt sediments were derived. Transparent yellow region denotes low resistivity, i.e. low velocity region, obtained through mapping of resistivity depth section using Eqs. (1a), (1b) and (2) to travel time. Average velocity in yellow region is 3 to 3.5 km/s.

consisting of stitched 1D inversions. However, the approximations allowed us to run the inversion process in a matter of minutes compared to hours of calculation needed if a true 2-D MT response were implemented in the calculation. The results show that our joint inversion concept, though simplified, yields an improvement in the inversion model and thus allows the delineation of sub-basalt sediments.

Using the physical property relationship that we have derived (Fig. 1) we convert the inversion results expressed in electrical resistivities to seismic velocities, hence we can calculate the two way travel time for the interfaces from the inversion result. As expected the supra-basalt layers match, as these are part of the starting model, but additionally we now recover an estimate for the base basalt. These are plotted on Fig. 2b as dashed lines. They do not precisely follow the base basalt reflection but it does map out the base of the highest resistivity anomalies.

5. SIMBA experiment

During the course of the EU-SIMBA project, a detailed MT experiment was conducted in the Faroe-Shetland Basin. Five marine MT instruments built for the project at the Universite de Bretagne Occidentale were used to record MT data at 17 stations along a profile that was coincident with the Flare-10 seismic reflection profile (White et al., 1999). Additional low frequency MT data at 4 sites have been

acquired using Woods Hole MT instruments. The position of the MT stations along the profile is marked by triangles on the map (Fig. 5). The seismic reflection data were processed to produce an image of the supra-basalt structures and the top basalt. For the real seismic data the processing included: source estimation and deconvolution; surface related multiple attenuation and tau-p filter (to suppress multiples); picking stacking velocity functions (every 2.5 km); top mute; stack; and migration. The velocity model to the top basalt derived from velocity analysis was simplified to produced a 2 layer sedimentary sequence with velocities of 1520 and 1995 m/s. These data were converted to resistivity values as a priori input using the relationships derived earlier (Eqs. (1a) and (1b)). The gravity data were extracted from the satellite free air database (Sandwell and Smith, 1997). The easternmost 12 MT stations which yielded highest quality MT data were provided for inversion. As for the synthetic example we fixed the upper layers from the a priori seismic data underlain by a 2 Ω m half-space. The 2D gravity and 1D MT joint inversion allowed for 9 layers including the half-space. The resulting resistivity section is shown in Fig. 5 and the observed and fitted data are presented in Fig. 6. The inversion result shows that a low resistivity section corresponding to a low velocity and low density region of 3 to 1 km thickness emerges underneath a basalt layer which itself has a thickness of approx. 1 to 2 km. The resistivity values suggest the presence of a sequence which is rich in sediments, thus to a phase of subsidence and sedimentation. The existence of sill in the sediments may not be inferred from

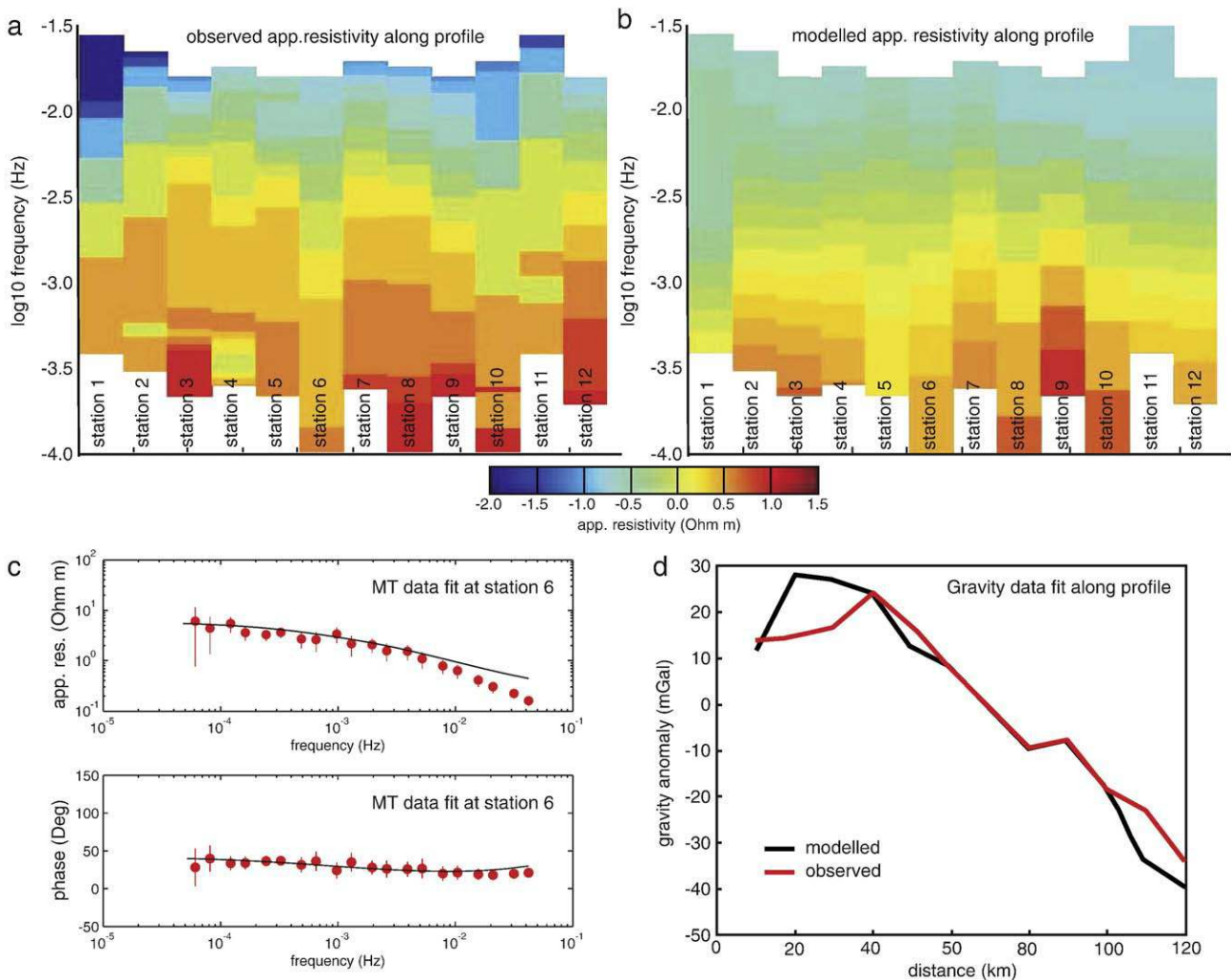


Fig. 6. (a) observed MT mode data of the 12 eastern most station along Flare10 profile. (b) MT response of the inversion model at these stations. (c) Example of data and fit at centre of profile. (d) Observed and modelled gravity response from inversion result.

resistivity values alone since their existence would not decrease the overall bulk resistivity sensed by MT measurements.

The bottom panel of Fig. 5 shows an overlay of the low velocity structure mapped to seismic travel time onto the seismic section. Because of the a priori use of the seismic data to constrain the upper layers, there is agreement between the model and the seismic data to the depth of top basalt. We believe the base of the basalt layer is congruent with reflectors seen in the seismic section as the reflections are probably from high-impedance sills intruded at or close to the base of the extrusive basalt sequence. The base of the model matches up with these reflection which gives confidence to our interpretation. Within the low velocity layer, intermittent reflectors point to the existence of interlayering, again probably caused by sills. From the resistivity/velocity relationship (Fig. 1) the velocity of this region is about 3 to 3.5 km/s. The existence and depth of the low velocity layer corresponds roughly to a low velocity region detected during the ISIMM experiment along a profile situated to the north of our profile (White et al., 2008), however the low velocity region along the iSIMM profile is with a thickness of 1 to 2 km slightly thinner and is characterized by a higher velocity of 4 to 4.2 km/s. Discrepancy between these parameters may be explained by the fact that the low velocity zone is not well resolved with seismic data alone or due to geological variations.

6. Discussion and conclusion

We have presented a concept of a joint inversion method that uses diverse data to constrain a common Earth model. For sub-basalt imaging we demonstrate that the combination of MT with gravity works provided any low resistivity layers above the basalt can be constrained using velocity structures derived from seismic data. The application of the joint inversion algorithm to different types of geophysical data sets of the Faroe shelf indicated the presence of a 1 to 3 km thick sediment layer underlying a 1 to 2 km thick basalt layer. The sediment layer may denote the location of a sedimented basin in the initial rift phase.

The key issues we have identified in this work are:

- gravity, MT and seismic data for sub-basalt sediment models contain complementary information that may be exploited through a joint inversion algorithm;
- the need to establish a relationship between the different physical properties. These are probably best defined empirically from wireline logging of nearby wells. For this initial work we have assumed simple relationships but for a more complete analysis the distributions of the cross-plots (Fig. 1) need to be included and analysed further;
- the mapping of the individual physical properties onto a common model, in this case we used resistivity; but equally we could have used either velocity or gravity;
- 1-D or quasi 2-D inversions are computationally efficient and we have obtained reasonable results for both synthetic and real data presented in this paper, proving the viability of this joint inversion approach. However for more complex targets with strong lateral heterogeneity or rough topography a full 2-D MT inversion needs to be incorporated and is currently being implemented;
- it is necessary to balance the relative strengths of the various data input in to the joint inversion to ensure that one data type does not

dominate the inversion, here we used ad-hoc scaling factors but a more reliable automated scheme needs to be developed for more extensive datasets;

- joint inversion presents a formal method to include diverse data in a common, robust model and helps interpretation by reducing the ambiguity from a range of models derived from single data sets.

Acknowledgements

We would like to acknowledge the SINDRI consortium for funding of the research presented. We also wish to acknowledge the crew of the MAGNUS HEINASON, Heri Ziska from the Faroese Geological Survey and Eli Christenson from the Faroese Fisheries Laboratory for their support in data acquisition and logistics, Adam Cherrett, TOTAL, for the finite-difference synthetic seismic data computed as part of the EU-SIMBA project and two anonymous reviewers for improving the manuscript. RWH was a NERC Advanced Fellow (2003–2008) NER/J/S/2002/00745.

References

- Cagniard, L., 1953. Basic theory of the magneto-telluric method of geophysical prospecting. *Geophysics* 37, 605–635.
- Gallardo, L.A., Meju, M.A., 2003. Characterization of heterogeneous near-surface materials by joint 2D inversion of dc resistivity and seismic data. *Geophys. Res. Lett.* vol. 30 (13), 1658. doi:10.1029/2003GL017370.
- Haber, E., Oldenburg, D., 1997. Joint inversion: a structural approach. *Inverse Probl.* 13, 63–77.
- Maresh, J., White, R.S., 2005. Seeing through a glass, darkly: strategies for imaging through basalt. *First Break* 23, 27–33.
- Martini, F.C., Bean, J., Khaksar, A., 2005. A complex 3D volume for subbasalt imaging'. *First Break* 23, 41–51.
- Musil, M., Maurer, H.R., Green, A., 2003. Discrete tomography and joint inversion for loosely connected or unconnected physical properties: application to crosshole seismic and georadar data sets. *Geophys. J. Int.* 153, 389–402.
- Peng, C., Toksoz, M.N., 1995. An optimal absorbing boundary condition for elastic wave modeling. *Geophysics* 60, 296.
- Price, A.T., 1962. The theory of magnetotelluric methods when the source field is considered. *Geophys. Res. Lett.* 67, 4309–4329.
- Sandwell, D.T., Smith, W.H.F., 1997. Marine gravity anomaly from Geosat and ERS 1 satellite altimetry. *J. Geophys. Res.* 102 (B5), 10039–10054.
- Schmutz, A., Albouy, Y., Guerin, R., Maquaire, O., Vassal, J., Schott, J.J., Decloitre, M., 2000. Joint electrical and time domain electromagnetism (TDEM) data inversion applied to the super sauze earthflow (France). *Surv. Geophys.* 21, 371–390.
- Tarits, P., 1984. *Algorithme de modélisation magnétotellurique en deux dimension*, PhD thesis, IPG, Paris, France.
- Telford, W.M., Geldart, L.P., Sheriff, R.E., Key, D.A., 1976. *Applied Geophysics*. Cambridge University Press, USA.
- Trinks, I., 2005. *Seismic tomography with a self-adaptive parameterization*, PhD thesis, Cambridge University, U.K.
- Vozoff, K., Jupp, D.L.B., 1975. Joint inversion of geophysical data. *Geophys. J. R. Astron. Soc.* 42, 977–991.
- White, R.S., Fruehn, J., Richardson, K.R., Cullen, E., Kirk, W., Smallwood, J.R., Latkiewicz, C., 1999. Faroes Large Aperture Research Experiment (FLARE): imaging through basalts. *Geology of the Northwest European Continental Margin*. Geological Society of London.
- White, R.S., Smith, L.K., Roberst, A.W., Christie, P.A.F., Kuznir, N.J., the rest of the iSIMM team, 2008. Lower crustal intrusion on the North Atlantic continental margin. *Nature* 452, 460–464. doi:10.1038/nature06687.
- Wyllie, M.R.J., Gregory, A.R., Gardner, G.H.F., 1958. An experimental investigation of factors affecting elastic wave velocities in porous media. *Geophysics* 23, 459–493.
- Wombell, R., Jones, E., Jakubowicz, H., Emsley, D., Boswell, P., Davis, P., 1999. Comparison of single-vessel and two-vessel long-offset acquisition. EAGE Annual Meeting, Helsinki.
- Ziolkowski, A., Hanssen, P., Gatliff, R., Jakubowicz, H., Dobson, A., Hampson, G., Li, X.Y., Liu, E.R., 2003. Use of low frequencies for sub-basalt imaging. *Geophys. Prospect.* 51 (3), 169–182.